



This is a repository copy of *1GHz clocked distribution of electrically generated entangled photon pairs*.

White Rose Research Online URL for this paper:
<https://eprints.whiterose.ac.uk/165348/>

Version: Submitted Version

Other:

Shooter, G, Xiang, Z-H, Müller, JRA et al. (11 more authors) (2020) 1GHz clocked distribution of electrically generated entangled photon pairs. UNSPECIFIED.

<https://doi.org/10.1364/oe.405466>

© 2020 The Author(s). For reuse permissions, please contact the Author(s).

Reuse

Items deposited in White Rose Research Online are protected by copyright, with all rights reserved unless indicated otherwise. They may be downloaded and/or printed for private study, or other acts as permitted by national copyright laws. The publisher or other rights holders may allow further reproduction and re-use of the full text version. This is indicated by the licence information on the White Rose Research Online record for the item.

Takedown

If you consider content in White Rose Research Online to be in breach of UK law, please notify us by emailing eprints@whiterose.ac.uk including the URL of the record and the reason for the withdrawal request.



eprints@whiterose.ac.uk
<https://eprints.whiterose.ac.uk/>

1GHz clocked distribution of electrically generated entangled photon pairs

G. Shooter,^{1,2} Z. Xiang,^{1,2} J.R.A. Müller,^{1,3} J. Skiba-Szymanska,¹ J. Huwer,^{1,*} J. Griffiths,² T. Mitchell,² M. Anderson,^{1,2} T. Müller,¹ A.B. Krysa,⁴ R. M. Stevenson,¹ J. Heffernan,⁴ D. A. Ritchie,² and A. J. Shields¹

¹*Toshiba Research Europe Limited, Cambridge Research Laboratory,
208 Cambridge Science Park, Milton Road,
Cambridge, CB4 0GZ, United Kingdom*

²*Cavendish Laboratory, University of Cambridge,
J.J. Thomson Avenue, Cambridge, CB3 0HE, United Kingdom*

³*Department of Physics and Astronomy,
University of Sheffield, Hounsfield Road, Sheffield S3 7RH, UK*

⁴*EPSRC National Epitaxy Facility, Department of Electronic & Electrical Engineering,
The University of Sheffield, 3 Solly Street, Sheffield, S1 4DE*

(Dated: 30/04/20)

Quantum networks are essential for realising distributed quantum computation and quantum communication. Entangled photons are a key resource, with applications such as quantum key distribution, quantum relays, and quantum repeaters. All components integrated in a quantum network must be synchronised and therefore comply with a certain clock frequency. In quantum key distribution, the most mature technology, the current standard clock rate is 1GHz. Here we show the first electrically pulsed sub-Poissonian entangled photon source compatible with existing fiber networks operating at this clock rate. The entangled LED is based on InAs/InP quantum dots emitting in the main telecom window, with a multi-photon probability of less than 10% per emission cycle and a maximum entanglement fidelity of 89%. We use this device to demonstrate GHz clocked distribution of entangled qubits over an installed fiber network between two points 4.6km apart.

* jan.huwer@crl.toshiba.co.uk

To perform high level operations [1–4] in a quantum network, entanglement must be distributed between nodes [5–8]. Intrinsic security of quantum communication protocols can be provided by entangled photon sources with sub-Poissonian statistics such as semiconductor quantum dots (QD)s [9, 10], unlike sources based on non-linear processes [11, 12].

Epitaxially grown semiconductor QDs can be readily incorporated into PIN diode structures, enabling the fabrication of light sources using standard semiconductor processing techniques [9, 13]. As QDs embedded within diodes can be electrically excited [14], it is possible to create entangled photon sources that can be conveniently operated similar to other standard light sources, such as telecom laser diodes. InAs/InP QDs emit in the lowest-loss silica fiber window [15], which makes them prime candidates for transmission over standard fiber networks.

Entangled LED (ELED) telecom C-band sources have been demonstrated with DC excitation [16]. Pulsed single [13, 17, 18] and entangled [9, 14, 19–22] photon sources based on semiconductor QDs have been developed but are either at short wavelengths, and therefore incompatible with existing fiber networks, or only operate at repetition rates too slow for current quantum network applications. Entanglement distribution experiments over installed networks have used low repetition rates [6–8] while GHz clock rates, necessary for synchronisation with standard quantum key distribution (QKD) systems, have only been demonstrated with Poissonian sources over long fiber in a laboratory [23, 24].

The fabrication of ELED devices used in this work was developed to be simple, with only two etch steps and two metal depositions. An image of a device is shown in figure 1(a). This design allows for fast electrical operation at GHz frequencies, with dimensions close to the limit imposed by the size of a bond ball as can be seen in figure 1(a). The ELED shows good electrical performance as a diode, with the resistance reaching 50Ω beyond the turn-on voltage. The wafer structure, described in Methods, is designed for QD emission in the telecom C-band. The emission spectrum shown in figure 1(b) comes from a QD that is located within a $5\mu\text{m}$ connected pillar, as can be seen in figure 1(a), and so can be readily relocated. The device was mounted onto the centre of a radio-frequency compatible FR4 packaging with conductive paint before wire bonding to a Au layer on one end of 50Ω impedance matched tracks, ending with a low-profile micro-coaxial connector as illustrated in the inset of figure 1(b).

In QDs, single photons are emitted via the radiative recombination of confined electron-

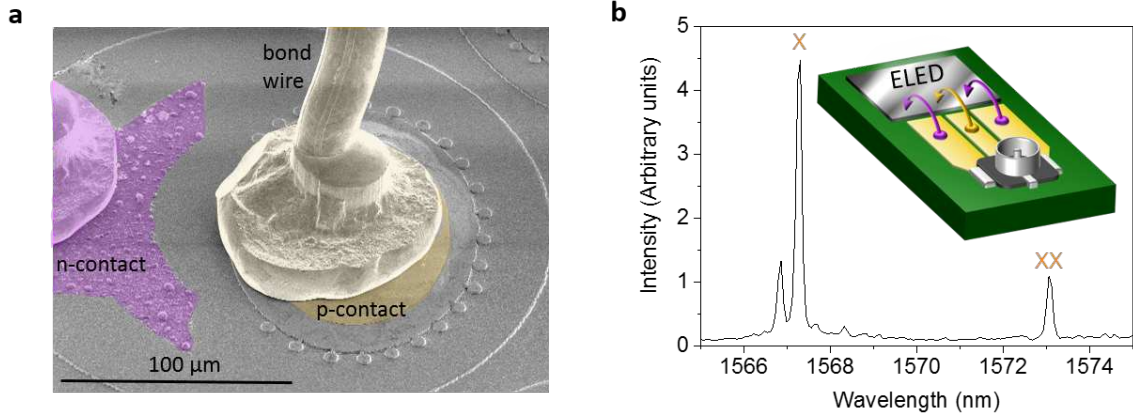


FIG. 1. A quantum dot LED for 1GHz pulsed electrical excitation. (a) A false colour scanning electron microscope image of a device; an oval mesa with connected pillars, electrically isolated from the surrounding wafer. (b) An electroluminescence (EL) spectrum of a quantum dot showing the exciton (X) and biexciton (XX) emission lines. The inset shows an illustration of the radio frequency compatible packaging; the ELED is wire bonded to impedance matched tracks (p-type and n-type bond are shown in yellow and purple respectively) which finish at a low-profile micro-coaxial connector.

hole (e-h) pairs [25]. Entangled photon pairs are emitted via the biexciton cascade [9] where a QD initialised in the doubly excited biexciton (XX) state decays to the singly excited exciton (X) state via emission of the first photon. This state subsequently decays via emission of a second photon, leaving the QD in the ground state. Due to conservation of angular momentum, the two emitted photons are maximally entangled in their polarization.

To assess the sub-Poissonian photon emission from the ELED, we measure the second order autocorrelation function ($g^{(2)}$) of X photons as shown in figure 2(a). This measurement requires isolation of the X spectral line as in figure 1(b). Since the QD emits at telecom wavelengths, a compact spectral wavelength filtering unit can be used that is based on an optical add-drop multiplexer as shown in figure 2(b) (FWHM $< 0.25\text{nm}$, 1.31dB loss), a common component in classical telecommunication technology.

The ELED was electrically driven with $\sim 130\text{ps}$ FWHM pulses with a high of 1.5V and a low of 0.3V; the arrival times of photons at each detector were recorded with respect to the 1GHz clock of these pulses. Photon correlations determined in postprocessing can be seen in figure 2(c). Coincidences in the 1ns squares along the diagonal are strongly suppressed

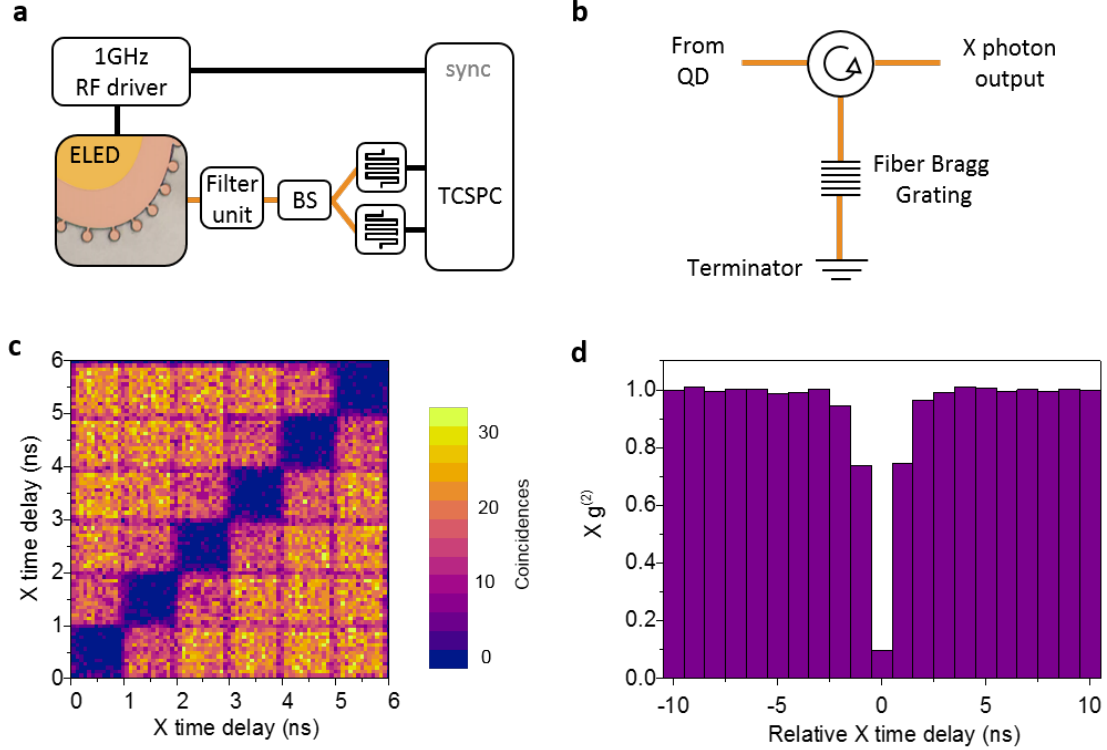


FIG. 2. Measurement of 1 GHz pulsed single photon emission. (a) Experimental setup for measuring the second order autocorrelation ($g^{(2)}$). Light from the ELED passes through a fiber-based spectral filter unit followed by a fiber 50:50 beam splitter (BS), with each output detected using superconducting nanowire single photon detectors and a time correlated single photon counter (TCSPC). (b) A diagram of the filter unit, with a circulator followed by a fiber bragg grating which reflects the X photons to the fiber output. (c) Time resolved coincidences of 1GHz clocked X photons for 6 consecutive emission cycles (72ps time bins) as a function of detection time with respect to the clock. (d) A histogram of normalised coincidences with 1ns bins for 21 relative time delays.

compared to the rest of the grid, corresponding to an excellent suppression of multi-photon emission within the same excitation cycle. The 1GHz pulsed operation of single photon emission can be clearly seen from the grid pattern with a 1ns period.

Photon coincidences in each 1ns square were normalised using coincidences in cycles with completely uncorrelated detection events. Figure 2(d) shows that the $g^{(2)}$ for X photons emitted in the same 1ns cycle is 0.097 ± 0.002 without application of any temporal post-selection. This is far below the classical limit, proving strongly sub-Poissonian emission.

As entangled photons are critical for quantum network applications, we now show the generation of 1GHz clocked entangled photon pairs from our ELED. The device was driven similarly to before, using pulses with a high of 1.5V and a low of 0.5V. The XX and X photons were separated with a spectral filter and each were detected with a polarization analyser comprising of an electronic polarisation controller (EPC) and a polarising beam splitter (PBS) followed by superconducting nanowire single photon detectors (SNSPD)s as in figure 3 (a). When detecting photons in a polarization basis PQ, P polarized XX photons were measured at detector 1 in figure 3(a), with X photons of P and Q polarizations measured at detectors 2 and 3 respectively. Photon arrival times for each detector with respect to the 1GHz clock signal divided by 64 were recorded with a time correlated single photon counter (TCSPC), with photon correlations and entanglement fidelity evaluated in postprocessing.

Photon pair correlations in the horizontal-vertical (HV) basis covering three consecutive excitation cycles can be seen in figure 3(b). Within a 1ns cycle both co (HH) and cross (HV) -polarized photon correlations are suppressed for time bins corresponding to the arrival of an X photon before a XX photon, due to the cascaded emission of the two photons of a pair. For time bins corresponding to the arrival of a XX photon before an X photon, only correlations for co-polarized photons are observed, as expected for the maximally entangled Bell ϕ^+ state. Importantly, correlations do not extend beyond each 1ns excitation cycle, verifying a clean reinitialisation of photon-pair emission at a 1GHz rate.

The resulting fidelity to the maximally entangled Bell ϕ^+ state, calculated as explained in Methods, is shown in figure 3(c). For most of the grid in figure 3(c), the entanglement fidelity is ~ 0.25 , corresponding to completely random polarization correlations. For XX and X photons from the same 1ns cycle, the entanglement fidelity rises above the classical limit of 0.5 for X photons arriving after XX photons, decaying with oscillations due to the fine structure splitting of the QD of $6.0\mu\text{eV}$.

Each vertical column of time bins in figure 3(c) contains photon coincidences with the same relative XX-X time delay, but different arrival times within the 1ns emission cycles. One can see that the entanglement fidelity drops for time bins at the start and end of the 1ns cycles due to reinitialisation of the emission ($\sim 130\text{ps}$). Therefore, to give an idea of the highest possible value, XX and X photon arrival times were additionally gated to 0.864ns around the center of 1ns cycles (shown as a white dashed box in figure 3(c)). The average of each column is plotted in figure 3(d), resulting in a maximum fidelity to the Bell ϕ^+ state

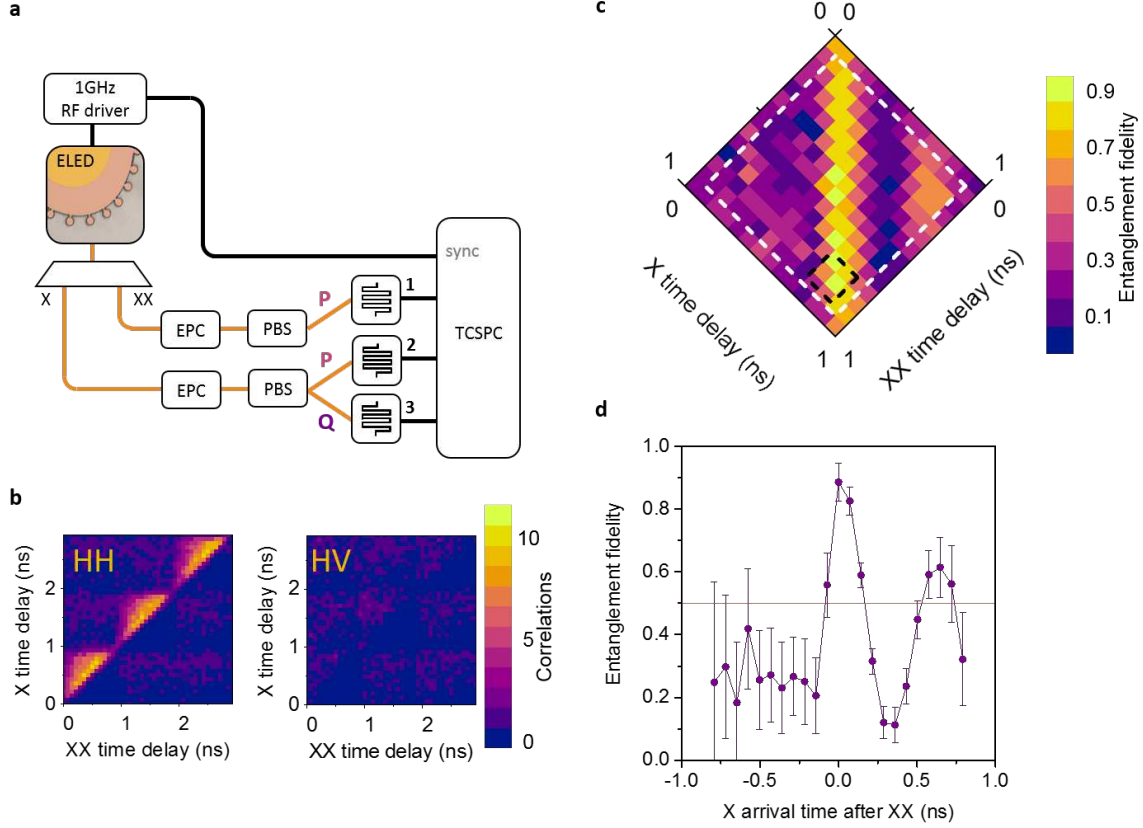


FIG. 3. Measurement of entanglement. (a) The experimental setup with a free-space spectral filter separating XX and X photons. Electronic polarization controllers (EPC)s followed by polarizing beam splitters (PBS)s set the detection polarization basis, with time correlated single photon counters (TCSPC)s recording photon arrivals at superconducting nanowire single photon detectors. (b) Photon correlations of horizontally (H) and vertically (V) polarized biexciton (XX) and exciton (X) photons, with (a) co- and (b) cross-polarized detection as a function of XX and X delay with respect to the 1GHz clock (72ps time bins). (c) The fidelity to the maximally entangled Bell ϕ^+ state with the same XX and X photon time bins as (b) but rotated by 135° . Photon arrival times gated to the central 0.864ns of each 1ns are shown by the dashed white square. A gate of 0.168ns is shown by the dashed black square. (d) The fidelity to the maximally entangled Bell ϕ^+ state as a function of relative delays between XX and X photons (72ps time bins). The horizontal orange line shows the classical limit of the entanglement fidelity.

of 0.89 ± 0.06 . However, this value corresponds to a bin size of 72ps, which is not compatible with post-selection free detection schemes.

Detectors used in state of the art QKD systems operating at 1GHz clock rates have typical

detection gate widths of $<170\text{ps}$ [26, 27]. To assess the performance of the pulsed ELED with these non-research grade detectors, we position a single 168ps integration window to give maximum entanglement fidelity, shown as a black dashed box in figure 3(c). This results in a fidelity of 0.86 ± 0.14 , in the regime compatible with error correction in quantum key distribution applications [28]. Analysing the X autocorrelation data from figure 2 in a similar fashion gives a $g^{(2)}$ of 0.05 ± 0.01 .

To demonstrate network compatibility of the pulsed entangled photon-pair source we distributed entanglement over 4.6km between the Toshiba Cambridge Research Laboratory (CRL) and the Physics Department of the University of Cambridge as shown in figure 4, using installed network fiber. The source was operated at CRL where X photons were detected, and XX photons were sent to a deployed detection system over 15km of installed fiber with 6dB loss at 1550nm .

The electrical 1GHz clock signal used to drive the ELED was down-sampled to 15.6MHz and converted to an optical signal at 1570nm and multiplexed with 1Gbit/s classical communication data traffic at 1310nm . The communication channel was required for remote control of the detection system and data acquisition, both classical signals were transmitted over a separate installed fiber. At the other end, both classical signals were demultiplexed, and the clock signal was converted back to an electrical signal to be used as the synchronisation reference in the deployed detection system.

In both locations, photon arrival times in two detector channels were recorded with respect to the reference clock with TCSPCs similar to the lab measurements previously discussed. Photon arrival times were measured in the three principal detection bases in sets of 7 minutes. Polarization drifts occurring over the network fiber due to changing environmental conditions were compensated for before each measurement using a similar stabilisation system as in [29]. Photon correlations were evaluated in postprocessing.

Entangled photon pairs were distributed between East and West Cambridge for 14 consecutive hours of operation. Figure 5 (a) and (b) shows results plotted in a similar way to figure 3 but for distribution of entanglement rather than a measurement in a laboratory. The maximum fidelity to the Bell ϕ^+ state, analysed on a 72ps grid with the reinitialisation period discarded as for the laboratory measurement, is 0.79 ± 0.03 . The 10% reduction in the fidelity when transmitting XX photons over the installed fiber is attributed to an increased ratio of background events to XX photon signal at the deployed detectors from $<2\%$ to

$>10\%$. Using the timing characteristics of GHz clocked detectors as indicated in figure 5(a), the maximum entanglement fidelity is 0.76 ± 0.06 . Figure 5(c) shows the evolution of the

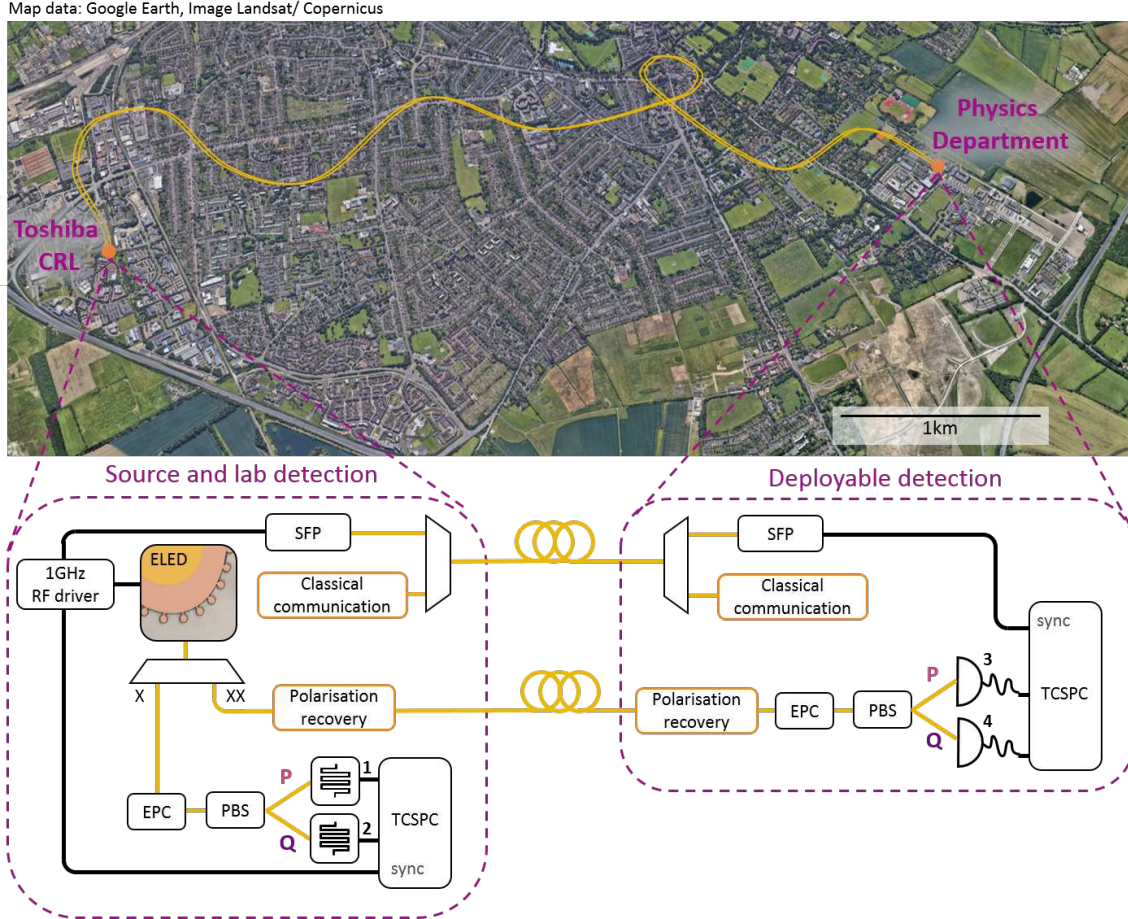


FIG. 4. Experimental setup for distribution of 1GHz clocked entangled photon pairs across the city of Cambridge. The entangled photon pairs were generated from an ELED at the Toshiba Cambridge Research Laboratory, with the X photons detected locally using detectors 1 and 2 (SNSPDs) and the XX photons detected at the Physics Department of the University of Cambridge with detectors 3 and 4 (APDs) in a deployed detection system. The detection polarization basis was set by EPCs followed by PBSs, with TCSPCs recording photon arrivals at detectors. When measuring photons in an arbitrary polarization basis PQ, detectors 1 and 3 measured P-polarized X and XX photons respectively and detectors 2 and 4 measured Q-polarized X and XX photons respectively. A polarization recovery system compensated for drifts occurring over the installed fiber. Classical communication for remote control of system components was multiplexed with the reference clock signal from a small form-factor pluggable transceiver (SFP) over a second fiber.

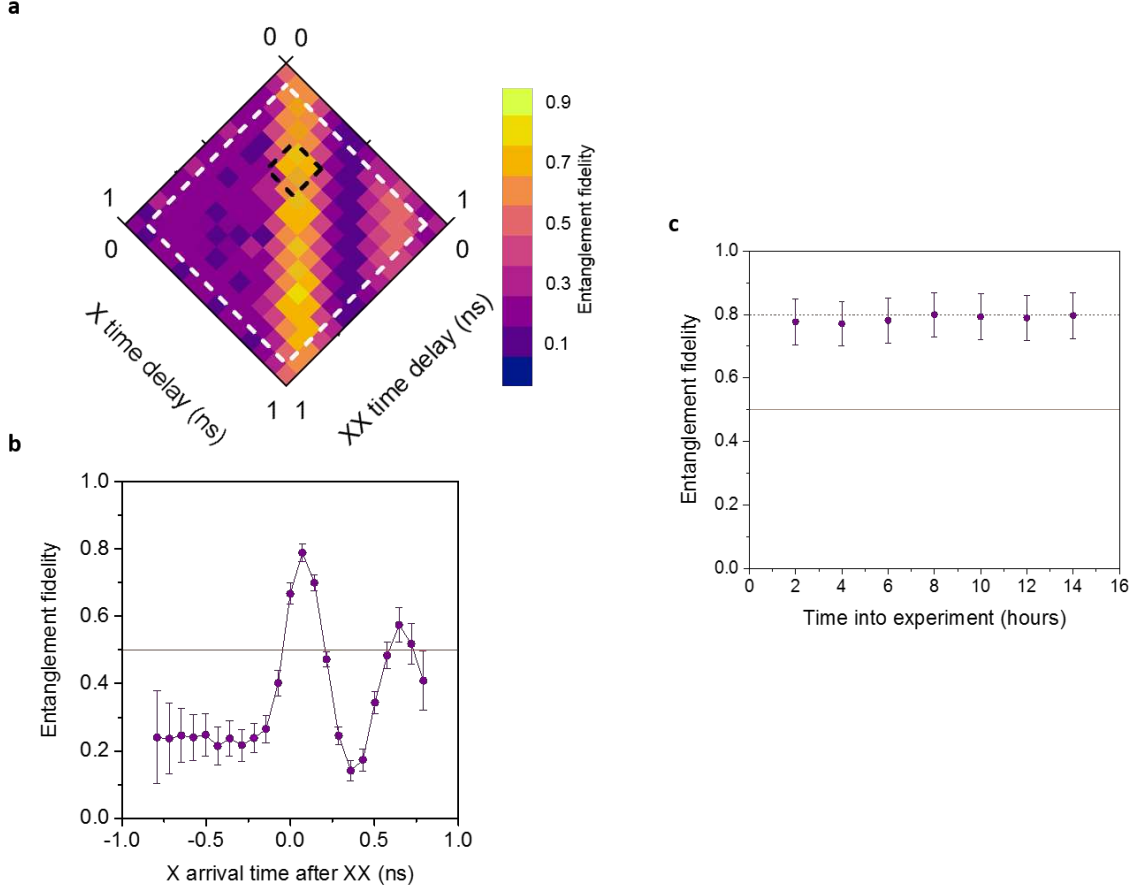


FIG. 5. Distribution of entangled photon pairs over 15km of installed fiber. (a) The fidelity to the maximally entangled Bell ϕ^+ state for 14 hours of data acquisition as a function of XX and X delay with respect to the 1GHz clock (72ps time bins) with gating applied similarly to in figure 3(c). (b) Fidelity as a function of relative delays between XX and X photons (72ps time bins). The horizontal orange line shows the classical limit of the entanglement fidelity. (c) The maximum entanglement fidelity from (a) for 2 hour sections throughout the experiment. The horizontal orange lines show the classical limit of the entanglement fidelity (solid) and a fidelity of 0.8 (dashed).

maximum entanglement fidelity for sets of 2 hours of data. It remains around 0.79 for the entire 14 hour experiment, demonstrating the excellent stability of the 1GHz clocked ELED as a source for distributed entangled photon pairs across a real-world fiber network.

We have shown an electrically driven 1GHz clocked telecom ELED with strong single photon characteristic, resulting in a two-photon probability of less than 10% without any temporal post-selection. Using the ELED as a source of 1GHz clocked entangled photons yields a maximum entanglement fidelity of 89%. In addition, the device is suitable for op-

eration using standard actively gated GHz clocked detector modules as are used in current QKD systems, with no additional software-based post-selection. Operation of the device in the lowest-loss telecom window enabled us for the first time to demonstrate the distribution of 1GHz clocked entangled qubits from a sub-Poissonian source on a city scale. The achieved entanglement fidelity of 79% proves reliability for electrically pulsed semiconductor quantum light sources connected to installed fiber networks. Pulsed operation with a common telecommunication clock frequency opens up the possibility for seamless integration with other quantum network hardware such as QKD systems and efficient time multiplexing with classical communication signals.

METHODS

Growth

The semiconductor wafer was grown by metal organic vapor phase epitaxy on an InP substrate. A bottom distributed Bragg reflector (DBR) comprising 20 layer pairs, each formed of 112nm of $((\text{Al}_{0.30}\text{Ga}_{0.70})_{0.48}\text{In}_{0.52}\text{As})$ and 123nm of InP were grown, with the top 3 repeats doped with $2 \times 10^{18} \text{cm}^{-3}$ of Si. InAs droplet QDs as in [15] were grown in a cavity on a $3\lambda/4$ intrinsic InP layer followed by a $5\lambda/4$ InP layer. The top nominal 150nm of the cavity was grown with Zn doping of $2 \times 10^{18} \text{cm}^{-3}$ to improve high speed electrical injection at low temperatures. 3 DBR pairs with Zn doping of $2 \times 10^{18} \text{cm}^{-3}$ and an InP capping layer completed the p-i-n diode structure.

Fabrication

The device in figure 1(a) was fabricated in 4 steps. To contact the p-layer, CrAu was thermally evaporated onto the wafer surface. The p-type contact was just large enough to fit a bond ball, $80 \times 110 \mu\text{m}$. The mesa and the isolated area were each etched using inductively coupled plasma (ICP) with Cl_2 based process chemistry. 150nm of AuGeNi was evaporated onto the isolated area to contact the n-layer before annealing at 420°C .

Characterisation

The device was cooled to 30K in a He vapour cryostat, with an xyz piezo nano-positioning stage enabling navigation around the device. A fibre-based confocal microscope system with NA 0.68 collected light emitted from the device. QD EL spectra were measured by sending this light via a fiber to a spectrometer with an InGaAs array. The fine structure splitting of a QD was measured as in [15], by polarization dependent spectroscopy using a quarter wave plate and linear polarizer in front of the spectrometer. This measurement identified XX and X lines, such as for the QD with the EL spectrum in figure 1(b) which had a fine structure splitting of $(6.0 \pm 0.3) \mu\text{eV}$.

Measurement of entanglement fidelity

XX and X photons emitted via the biexciton cascade are co-polarized in the horizontal/vertical basis due to conservation of angular momentum [9]. The degree of correlation in a polarization basis PQ is calculated from co-polarized, c_{PP} , and cross-polarized, c_{PQ} , photon correlations by

$$C_{PQ} = \frac{c_{PP} - c_{PQ}}{c_{PP} + c_{PQ}}.$$

The entanglement fidelity to the maximally entangled Bell ϕ^+ state

$$f = \frac{1 + C_{HV} + C_{DA} - C_{RL}}{4},$$

is obtained [30] from measurements in the horizontal/vertical (HV), diagonal/antidiagonal (DA), and right- and left-hand circularly polarized (RL) detection bases. A free-space spectral filter was used to separate XX and X photons in the entanglement measurements in figures 3, 4, and 5, followed by electronic polarization controllers and polarizing beam splitters before the detectors.

Entanglement distribution photon detection

At CRL, the overall timing jitter for detection was 70ps including the superconducting nanowire single photon detectors (SNSPD)s (Single Quantum). In the deployed system, the overall timing jitter for detection was around 75ps including the avalanche photodiodes (APD)s. The combined X photon rate at the SNSPDs, detectors 1 and 2 in figure 4, was around 190 000 cps and the combined XX photon rate at the APDs, detectors 3 and 4 in figure 4, was around 15 000 cps.

To calibrate the detection basis, the QD emission was replaced by a polarization reference matched to the eigenbasis of emitted photon pairs (not shown in figure 4). EPC voltages were then varied to minimise the output signal from one output mode of the PBS at a detector, aligning the detection basis to the reference.

ACKNOWLEDGEMENTS

The authors acknowledge partial financial support from the Engineering and Physical Sciences Research Council and the UK's innovation agency, Innovate UK. G. Shooter and M. Anderson acknowledge support from Industrial CASE awards funded by the EPSRC and Toshiba Research Europe Limited. Z.-H. Xiang acknowledges support from the Cambridge Trust and China Scholarship Council (CSC). J.R.A. Müller acknowledges support from the European Union's Horizon 2020 research and innovation programme under the Marie Skłodowska-Curie grant agreement No 721394.

-
- [1] A. K. Ekert, “Quantum cryptography based on bell’s theorem,” *Physical review letters*, vol. 67, no. 6, p. 661, 1991.
- [2] H.-J. Briegel, W. Dür, J. I. Cirac, and P. Zoller, “Quantum repeaters: the role of imperfect local operations in quantum communication,” *Physical review letters*, vol. 81, no. 26, p. 5932, 1998.
- [3] B. C. Jacobs, T. B. Pittman, and J. D. Franson, “Quantum relays and noise suppression using linear optics,” *Physical Review A*, vol. 66, no. 5, p. 052307, 2002.
- [4] H. de Riedmatten, I. Marcikic, W. Tittel, H. Zbinden, D. Collins, and N. Gisin, “Long distance quantum teleportation in a quantum relay configuration,” *Physical review letters*, vol. 92, no. 4, p. 047904, 2004.
- [5] P. Komar, E. M. Kessler, M. Bishof, L. Jiang, A. S. Sørensen, J. Ye, and M. D. Lukin, “A quantum network of clocks,” *Nature Physics*, vol. 10, no. 8, p. 582, 2014.
- [6] Q.-C. Sun, Y.-L. Mao, S.-J. Chen, W. Zhang, Y.-F. Jiang, Y.-B. Zhang, W.-J. Zhang, S. Miki, T. Yamashita, H. Terai, *et al.*, “Quantum teleportation with independent sources and prior entanglement distribution over a network,” *Nature Photonics*, vol. 10, no. 10, pp. 671–675, 2016.
- [7] R. Valivarthi, Q. Zhou, G. H. Aguilar, V. B. Verma, F. Marsili, M. D. Shaw, S. W. Nam, D. Oblak, W. Tittel, *et al.*, “Quantum teleportation across a metropolitan fibre network,” *Nature Photonics*, vol. 10, no. 10, p. 676, 2016.
- [8] S. Wengerowsky, S. Joshi, F. Steinlechner, J. Zichi, S. Dobrovolskiy, R. van der Molen, J. Los, V. Zwiller, M. Versteegh, A. Mura, D. Calonico, M. Inguscio, H. Hübel, L. Bo, T. Scheidl, A. Zeilinger, A. Xuereb, and R. Ursin, “Entanglement distribution over a 96-km-long submarine optical fiber,” *Proceedings of the National Academy of Sciences*, vol. 116, no. 14, pp. 6684–6688, 2019.
- [9] O. Benson, C. Santori, M. Pelton, and Y. Yamamoto, “Regulated and entangled photons from a single quantum dot,” *Physical review letters*, vol. 84, no. 11, p. 2513, 2000.
- [10] P. Michler, A. Imamoglu, M. D. Mason, P. J. Carson, G. F. Strouse, and S. K. Buratto, “Quantum correlation among photons from a single quantum dot at room temperature,” *Nature*, vol. 406, no. 6799, p. 968, 2000.

- [11] P. G. Kwiat, K. Mattle, H. Weinfurter, A. Zeilinger, A. V. Sergienko, and Y. Shih, “New high-intensity source of polarization-entangled photon pairs,” *Physical Review Letters*, vol. 75, no. 24, p. 4337, 1995.
- [12] X. Li, P. L. Voss, J. E. Sharping, and P. Kumar, “Optical-fiber source of polarization-entangled photons in the 1550 nm telecom band,” *Physical Review Letters*, vol. 94, no. 5, p. 053601, 2005.
- [13] P. Michler, A. Kiraz, C. Becher, W. V. Schoenfeld, P. M. Petroff, L. Zhang, E. Hu, and A. Imamoglu, “A quantum dot single-photon turnstile device,” *science*, vol. 290, no. 5500, pp. 2282–2285, 2000.
- [14] Z. Yuan, B. E. Kardynal, R. M. Stevenson, A. J. Shields, C. J. Lobo, K. Cooper, N. S. Beattie, D. A. Ritchie, and M. Pepper, “Electrically driven single-photon source,” *science*, vol. 295, no. 5552, pp. 102–105, 2002.
- [15] J. Skiba-Szymanska, R. M. Stevenson, C. Varnava, M. Felle, J. Huwer, T. Müller, A. J. Bennett, J. P. Lee, I. Farrer, A. B. Krysa, *et al.*, “Universal growth scheme for quantum dots with low fine-structure splitting at various emission wavelengths,” *Physical Review Applied*, vol. 8, no. 1, p. 014013, 2017.
- [16] T. Müller, J. Skiba-Szymanska, A. B. Krysa, J. Huwer, M. Felle, M. Anderson, R. M. Stevenson, J. Heffernan, D. A. Ritchie, and A. J. Shields, “A quantum light-emitting diode for the standard telecom window around 1,550 nm,” *Nature communications*, vol. 9, no. 1, p. 862, 2018.
- [17] C. Santori, M. Pelton, G. Solomon, Y. Dale, and Y. Yamamoto, “Triggered single photons from a quantum dot,” *Physical review letters*, vol. 86, no. 8, p. 1502, 2001.
- [18] F. Hargart, C. A. Kessler, T. Schwarzbäck, E. Koroknay, S. Weidenfeld, M. Jetter, and P. Michler, “Electrically driven quantum dot single-photon source at 2 ghz excitation repetition rate with ultra-low emission time jitter,” *Applied Physics Letters*, vol. 102, no. 1, p. 011126, 2013.
- [19] R. M. Stevenson, R. J. Young, P. Atkinson, K. Cooper, D. A. Ritchie, and A. J. Shields, “A semiconductor source of triggered entangled photon pairs,” *Nature*, vol. 439, no. 7073, p. 179, 2006.
- [20] J. Zhang, J. S. Wildmann, F. Ding, R. Trotta, Y. Huo, E. Zallo, D. Huber, A. Rastelli, and O. G. Schmidt, “High yield and ultrafast sources of electrically triggered entangled-photon pairs based on strain-tunable quantum dots,” *Nature communications*, vol. 6, p. 10067, 2015.

- [21] C. Varnava, R. M. Stevenson, J. Nilsson, J. Skiba-Szymanska, B. Dzurňák, M. Lucamarini, R. V. Penty, I. Farrer, D. A. Ritchie, and A. J. Shields, “An entangled-led-driven quantum relay over 1 km,” *npj Quantum Information*, vol. 2, p. 16006, 2016.
- [22] J. R. Müller, R. M. Stevenson, J. Skiba-Szymanska, G. Shooter, J. Huwer, I. Farrer, D. A. Ritchie, and A. J. Shields, “Active reset of a radiative cascade for superequilibrium entangled photon generation,” *arXiv preprint arXiv:2001.06251*, 2020.
- [23] T. Honjo, H. Takesue, H. Kamada, Y. Nishida, O. Tadanaga, M. Asobe, and K. Inoue, “Long-distance distribution of time-bin entangled photon pairs over 100 km using frequency up-conversion detectors,” *Optics express*, vol. 15, no. 21, pp. 13957–13964, 2007.
- [24] T. Inagaki, N. Matsuda, O. Tadanaga, M. Asobe, and H. Takesue, “Entanglement distribution over 300 km of fiber,” *Optics express*, vol. 21, no. 20, pp. 23241–23249, 2013.
- [25] A. Imamoglu, Y. Yamamoto, *et al.*, “Turnstile device for heralded single photons: Coulomb blockade of electron and hole tunneling in quantum confined p-i-n heterojunctions,” *Physical review letters*, vol. 72, no. 2, p. 210, 1994.
- [26] Z. Yuan, B. Kardynal, A. Sharpe, and A. Shields, “High speed single photon detection in the near infrared,” *Applied Physics Letters*, vol. 91, no. 4, p. 041114, 2007.
- [27] Z. Yuan, A. Dixon, J. Dynes, A. Sharpe, and A. Shields, “Gigahertz quantum key distribution with ingaas avalanche photodiodes,” *Applied Physics Letters*, vol. 92, no. 20, p. 201104, 2008.
- [28] H. Chau, “Practical scheme to share a secret key through a quantum channel with a 27.6% bit error rate,” *Physical Review A*, vol. 66, no. 6, p. 060302, 2002.
- [29] Z.-H. Xiang, J. Huwer, J. Skiba-Szymanska, R. Stevenson, D. Ellis, I. Farrer, M. Ward, D. Ritchie, and A. Shields, “A tuneable telecom-wavelength entangled light emitting diode,” *arXiv preprint arXiv:1909.12222*, 2019.
- [30] M. B. Ward, M. C. Dean, R. M. Stevenson, A. J. Bennett, D. J. Ellis, K. Cooper, I. Farrer, C. A. Nicoll, D. A. Ritchie, and A. J. Shields, “Coherent dynamics of a telecom-wavelength entangled photon source,” *Nature communications*, vol. 5, p. 3316, 2014.